



Investigation of pH evolution with Cr(VI) removal in electrocoagulation process: Proposing a real-time control strategy



Hai-yin Xu, Zhao-hui Yang*, Guang-ming Zeng, Yuan-ling Luo, Jing Huang, Li-ke Wang, Pei-pei Song, Xi Mo

College of Environmental Science and Engineering, Hunan University, Changsha 410082, PR China

Key Laboratory of Environmental Biology and Pollution Control (Hunan University), Ministry of Education, Changsha 410082, PR China

H I G H L I G H T S

- A theory of the relationships between initial pH and chromic alkalinity for final pH was built.
- Final pH was conditioned by initial pH and chromic alkalinity rather than current density.
- The final pH can be detected by the features of pH evolution when $p[\text{Cr(VI)}] = \text{pH}_i$ and $p[\text{Cr(VI)}] < \text{pH}_i$.
- A real-time control strategy for fluctuant (or stable) Cr(VI) wastewater treatment was proposed.

A R T I C L E I N F O

Article history:

Received 5 August 2013

Received in revised form 16 October 2013

Accepted 7 November 2013

Available online 15 November 2013

Keywords:

Electrocoagulation

Final pH

Cr(VI) removal

Real-time control strategy

A B S T R A C T

The pH value is easily monitored and widely used in real-time control processes. It is also a key parameter in removing Cr(VI) during electrocoagulation. We developed a theory of relations between initial pH (pH_i) and chromic alkalinity ($p[\text{Cr(VI)}]$), and the final pH of a solution. That was, when $p[\text{Cr(VI)}] = \text{pH}_i$, the final pH was neutral; when $p[\text{Cr(VI)}] < \text{pH}_i$, the final pH was alkaline; and when $p[\text{Cr(VI)}] > \text{pH}_i$, the final pH was acidic. Response surface methodology confirmed that final pH was influenced by initial pH and initial Cr(VI) concentration rather than by current density. Subsequently, the relationship between pH evolution and Cr(VI) removal was investigated for the aforementioned final pH conditions. Our results suggested that the point of final pH can be detected by the features of pH evolution in case of $p[\text{Cr(VI)}] = \text{pH}_i$ and $p[\text{Cr(VI)}] < \text{pH}_i$. Rapid Cr(VI) removal rate was achieved when $p[\text{Cr(VI)}] > \text{pH}_i$. However, the major fraction of dissolved Cr(III) and the uncertain point of final pH were observed in this condition. Finally, we proposed a real-time control strategy for treating fluctuant (or stable) Cr(VI)-contaminated wastewater based on the features of pH evolution.

© 2013 Elsevier B.V. All rights reserved.

1. Introduction

Regulatory demands for decreasing Cr(VI) discharge in any chemical form are becoming stricter and will continue to do so until this pollutant in wastewater is completely abated [1]. Consequently, it leads to the increase of the cost of corresponding infrastructure investments and operation [2]. As a result, several electrochemical processes such as electrocoagulation (EC) [2–7], electrocoagulation-electrofloatation [8], electrodialysis [9–11], and electrodeionization [12], have been developed. EC, a process of generating metal coagulants electrochemically, is suitable for treating Cr(VI)-contaminated wastewater because of its

advantages over traditional chemical treatment methods. Such advantages include no chemical requirement, minimal sludge production, and negligible process control [2,3,6]. As such, EC is one of the technologies used in reducing Cr(VI) discharges in the Xiangjiang River in Hunan Province. A 50% reduction in Cr(VI) emissions compared with the 2008 level is one of the objectives of the “12th Five-year Plan”, a comprehensive project for preventing and controlling heavy metal pollution in Hunan Province by 2015 [13].

EC process with sacrificial iron anodes (Fe-EC) has been extensively investigated on Cr(VI) removal [2–7]. Notably, the Fe-EC performance is influenced by many factors such as initial pH [6], current density [14], treatment time [15], and electrolytes [16]. In addition, the varying practices in the production process may cause the fluctuations of Cr(VI) wastewater from the workshop. Hence, the implementation of field-scale EC systems usually operates under continuous and excess current supply conditions, which results in a superfluous iron materials and electric energy

* Corresponding author at: College of Environmental Science and Engineering, Hunan University, Changsha 410082, PR China. Tel.: +86 15717484818; fax: +86 0731 88822829.

E-mail address: yzh@hnu.edu.cn (Z.-h. Yang).

consumption. But fortunately, some authors have proposed that the real-time control process, operating with online monitoring by specific index (such as pH, ORP, and DO), offers many advantages such as self-adjusted to various treatment conditions and energy savings [17–19]. Now that detailed researches on real-time process control strategy in EC systems are scarce, a proper monitoring and control index appears to be the major issue for this process.

Many reports have suggested that the pH is one of the widest used control parameters in determining the termination points [18,19]. It is also a key parameter in removing Cr(VI) during EC process [16]. As observed by other investigators, the EC treatment induces a pH increase from acidic to more basic condition [14,20]. Consequently, EC process is efficient in removing Cr(VI) pollutants from wastewater, since the reduction of Cr(VI) to Cr(III) by Fe(II) is preferred to occur in acidic conditions, and the coagulation of Fe(III) and Cr(III) is favorable in alkali conditions [16]. However, the presence of high concentration of proton (H^+) can be disadvantageous for precipitation of Fe(III)/Cr(III) hydroxides [8]. Furthermore, the iron hydroxide flocs have been reported to hardly float up in a highly alkaline environment, due to their flocs are small and dense [3,8,21]. Thus the optimum condition of Cr(VI) removal in EC process is by virtue of regulating final pH at neutral rather than acidic and alkaline.

Therefore, understanding the factors that influence final pH and quantifying the relationships among these factors are essential. Nevertheless, this topic is not available in current literature. Most studies focused on the mechanisms of pH evolution during EC. The following summary of Fe-EC for Cr(VI) removal reported in literature demonstrates the ambiguity of pH evolution mechanisms involved in the process.

- (1) Direct effect. Some studies show that the bulk solution pH would increase in acidic condition, which is due to hydroxyl ions produced at the cathode [4,16]. In contrast, others report the precipitation of metallic species consumes the alkalinity produced at the cathode, thereby resulting in an invariability of pH under alkaline conditions [3,21]. Meanwhile, Mouedhen et al. suggest the pH variation is essentially attributed to combined effect of hydroxyl ions produced at the cathode and hydroxide precipitate of $Cr(OH)_3$ and $Fe(OH)_3$ [7]. Additionally, many consider the solution pH depends on the initial pH [6,16,20].
- (2) Indirect effect. Numerous studies have reported that operating parameters, such as electric current and electrolytes enhance anode dissolution, thus causing an increase in the pH of solutions [6,20]. In addition, CO_2 gas transfer has also been reported to lead to pH increase in solutions [22]. Moreover, chloride and sulphate ions in the solution make only a slight difference to the solubility equilibrium of Fe, and the magnitude of the increase of solubility due to the formation of complexes is very small compared with the change of pH [16].

Additionally, some temporary effects can also influence the pH value. The immediate or time lag of pH during EC process has been noticed by Lakshmanan et al. [23]. Fortunately, the influence of this may be eliminated by some operation methods.

The effects of the above factors towards final pH in the quoted studies are unknown but certainly crucial factors. Therefore, the aims of this study were to (1) find out the influencing factors on final pH of Cr(VI) removal and determined their quantitative relations; (2) confirm the above results by response surface methodology (RSM) experiment; (3) investigate the pH evolution in different final pH conditions (acidic, neutral and alkaline) and based on that, and (4) propose a real-time control strategy.

2. Material and methods

2.1. Experimental set-up

Experiments were conducted in a 2.5 L EC reactor (Fig. 1) using 1.5 cm diameter reagent-grade iron rod (99.5% Fe) with active surface area of 16 cm^2 . The distance between the anode and cathode was 25 mm. The electrodes, precleaned mechanically with sandpaper to remove any passive film, were connected to a programmable DC power supply (RIGOL DP1116A, China, maximum 32,000V and 10,000A) which controlled by user-defined programming. Synthetic solutions containing Cr(VI) were prepared by dissolving reagent grade $K_2Cr_2O_7$ into deionized water, and analytical grade anhydrous NaCl was added as a supporting electrolyte to avoid iron passivation in the EC process [16]. A magnetic stirrer with stirring rate of about 300 rpm was used during the electrolysis to ensure adequate mixing. Samples (30 mL) were taken from the reactor using a wide-tipped syringe based on the requirement of the experimental object. A first set of samples was filtered through $0.45\ \mu\text{m}$ nylon filters for the determination of Cr(VI) and Cr(Tot). A second set of unfiltered samples was taken and digested in HNO_3 before analysis for the determination of Fe(II) and Fe(Tot). The dissolved oxygen (DO) was measured by DO meter (HI 98186, HANNA, Italy). The pH of the solutions was measured by pH meter (HI 98184, HANNA, Italy) and adjusted by adding 0.5 M NaOH or HNO_3 solutions. The pH value was measured in pH monitoring room by peristaltic pump to guaranteeing precision. All experiments were conducted at room temperature ($23 \pm 2\ ^\circ\text{C}$).

2.2. Analytical methods

Cr(VI) concentration was measured with a 721 spectrophotometer (Shanghai, China) using the standard method of the diphenylcarbazide [24]. Cr(Tot) and Fe(Tot) concentrations were analyzed using flame atomic absorption spectroscopy (AAS) [24]. The Fe(II) concentration was determined by UV spectrophotometry using the 1,10 phenanthroline method [25]. The Fe(III) concentration was then calculated from the difference between Fe(Tot) and Fe(II).

2.3. Equilibrium modeling

The Visual MINTEQ ver. 3.0. was used to determine the possible species formed [26]. Solution speciation was calculated using thermodynamic data and equilibrium constants of the Visual MINTEQ

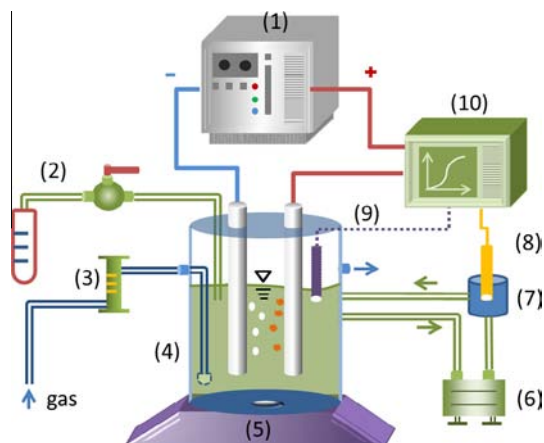


Fig. 1. Schematic process and arrangement with pH monitoring system (1) DC power; (2) sample collection; (3) gas-flow meter; (4) EC reactor; (5) magnetic stirrer; (6) peristaltic pump; (7) pH monitoring room; (8) pH probe; (9) DO probe; and (10) computer.

database, which mostly relies on the NIST Critical Stability constants database (database NIST 46.7) [27]. We used the Davies equation for activity correction and van't Hoff's equation for temperature correction [28].

Total Cr(VI), Cr(III), Fe(III) and Fe(II) in the Visual Minteq runs was set to 2, 2, 6 and 6 mM, respectively, and Cr(III), Fe(III), Fe(II) was allowed to precipitate when the solubility product for $\text{Cr}(\text{OH})_3(\text{s})$ (with $\log K_s = -0.49$, $\Delta H_r = -110.5$ at 25 °C), $\text{Fe}(\text{OH})_3$ (with $\log K_s = 3.2$, $\Delta H_r = -100.4$ kJ/mol at 25 °C), $\text{Fe}(\text{OH})_2(\text{s})$ (with $\log K_s = 13.49$ kJ/mol, $\Delta H_r = -91.62$ kJ/mol at 25 °C) was exceeded, respectively.

2.4. Calculations

The theoretically dissolve amounts of ferrous from Faraday's law (Eq. (1)). Faraday's formula could be expressed as:

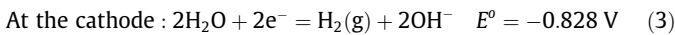
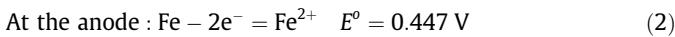
$$\Delta m_{\text{theo}} = \frac{M \cdot I \cdot \Delta t}{n \cdot F} \quad (1)$$

where I is the current (A), Δt is the intervals time (s), Δm_{theo} is the amount of iron dissolved (g), M is the atomic weight of the iron (56 g/mol), n is the number of electron moles ($n = 2$, in Eq. (2)) and F is the Faraday's constant ($F = 96,487$ C/mol).

2.5. Theory of Cr(VI) removal-pH evolution

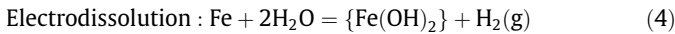
2.5.1. Basic concept of EC process

Concerning iron material, the main electrochemical reactions occurring at electrode surfaces during electrolysis are [29]:



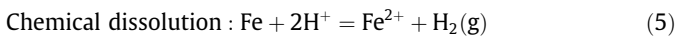
The pH, at the vicinity of the anode, is more acidic than the bulk, since the ferrous electrodisolved from anode (Eq. (2)) is immediately hydrolyzing and releasing hydrogen ions [7]. But cathode vicinity is more alkaline than the bulk according to the Eq. (3).

The overall electrodisolution reaction (combination of anode Eq. (2) and cathode Eq. (3)) can be expressed as follow:

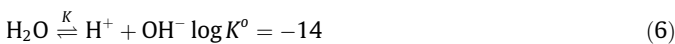


where $\{\text{Fe}(\text{OH})_2\}$ represents the neutral products in bulk solution, such as $\text{Fe}(\text{OH})_2(\text{s})$, $\text{Fe}(\text{OH})^+ + \text{OH}^-$, and $\text{Fe}^{2+} + 2\text{OH}^-$, depending on pH (Fig. 2).

During the acidic solution, chemical dissolution occurs.



An ionization equilibrium reaction of H_2O happens under acidic condition:



Substituting Eqs. (5) and (6), we also obtain Eq. (4).

Above all, $\{\text{Fe}(\text{OH})_2\}$ was used in this study to represent the neutral products generated during electrodisolution and chemical dissolution process.

2.5.2. Mechanisms for Cr(VI) removal in EC process

Cr(VI) removal by Fe-EC process contains several mechanisms:

- (1) Chemical reduction [7,14,16,20,30,31]: the reduction of Cr(VI) to Cr(III) by the Fe^{2+} ions generated from electrodisolution and chemical dissolution, is the predominant way for Cr(VI) removal.

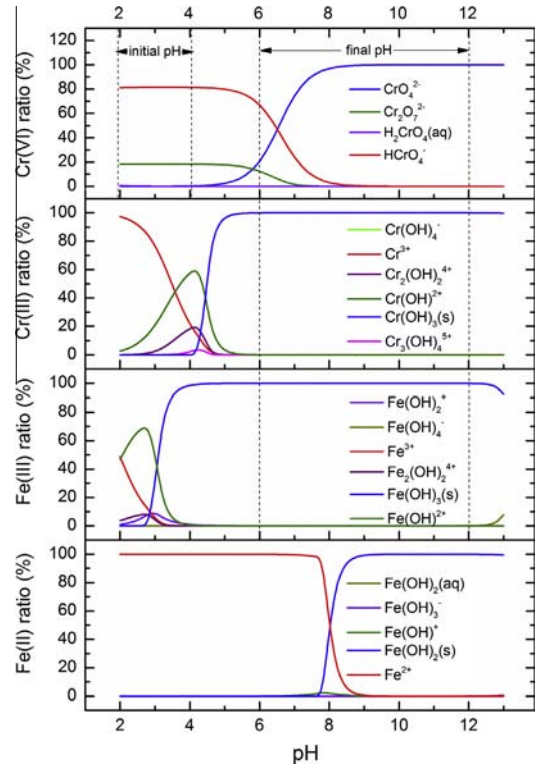
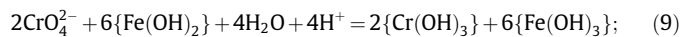
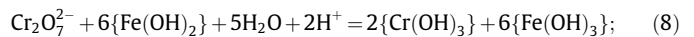
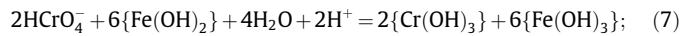
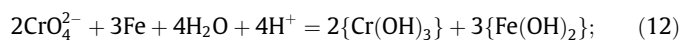
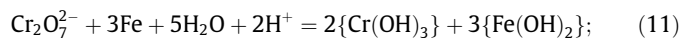
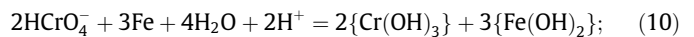


Fig. 2. Predominance zone diagram for Cr(VI) species, Cr(III), Fe(III) and Fe(II) ratio in solution simulated by Visual MINTEQ ver. 3.0.

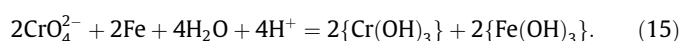
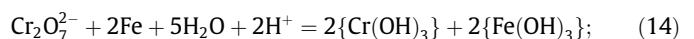
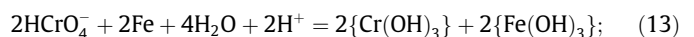
In our experiments described previously (Section 2.5.1), the $\{\text{Fe}(\text{OH})_2\}$ was used to indicate the iron species produced by EC process. Therefore, we obtained the following equations:



- (2) Cathode reduction [3,14,32,33]: the electrochemical reduction of Cr(VI) directly at the cathode, then the generated $\{\text{Fe}(\text{OH})_2\}$ is consumed by Cr(VI) with chemical reduction (Eqs. (10)–(12)).



- (3) Zero-valent iron reduction [3,4,34]: in the acidic conditions, Cr(VI) can be reduced at anode surface by zero-valent iron.



where $\{\text{Cr}(\text{OH})_3\}$ and $\{\text{Fe}(\text{OH})_3\}$ are the products of EC, which exists in aqueous medium as neutral species, for instance, $\text{Cr}(\text{OH})_3(\text{s})$,

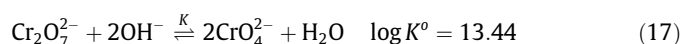
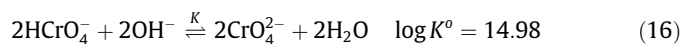
$\text{Cr}(\text{OH})_4^- + \text{H}^+$, $\text{Cr}_3(\text{OH})_4^{5+} + 5\text{OH}^-$, $\text{Fe}(\text{OH})_3(\text{s})$, $\text{Fe}(\text{OH})_2^- + \text{H}^+$, and $\text{Fe}^{3+} + 3\text{OH}^-$, etc., depending on solution pH (Fig. 2).

2.5.3. Reaction stoichiometry of Cr(VI) and protons (H^+)

In this section, some important assumptions were given in the following:

- (1) In the pH range of 2.0–4.0, Cr(VI) only existed in bulk solution as the species of HCrO_4^- and $\text{Cr}_2\text{O}_7^{2-}$. This was consistent with the data shown in Fig. 2, the ratio of H_2CrO_4 and CrO_4^{2-} was below 0.5% and 0.25%, respectively. Therefore, the species of H_2CrO_4 and CrO_4^{2-} could be ignored in this situation.
- (2) At the end of Cr(VI) removal, no $\{\text{Fe}(\text{OH})_2\}$ was residual in the bulk solution, and the final pH was between 5.0 and 12.0. Hence the products of $\{\text{Cr}(\text{OH})_3\}$ and $\{\text{Fe}(\text{OH})_3\}$ exist as $\text{Cr}(\text{OH})_3(\text{s})$ and $\text{Fe}(\text{OH})_3(\text{s})$, respectively (Fig. 2).

Obviously, HCrO_4^- and $\text{Cr}_2\text{O}_7^{2-}$ were removed by the route of I (Eqs. (7), (10), and (13)) and II (Eqs. (8), (11), and (14)), respectively. Given the stoichiometry of these reactions, 2 mol Cr(VI) from HCrO_4^- or $\text{Cr}_2\text{O}_7^{2-}$ were reduced accompanying with 2 mol protons, and resulting in the formation of 2 mol $\text{Cr}(\text{OH})_3(\text{s})$. It means that 1 mol Cr(VI) reduction requires 1 mol protons. When pH above 6.5, the CrO_4^{2-} dominated in bulk solution (Fig. 2). With regard to the route of III, it consisted of two parts: the transformation of HCrO_4^- and $\text{Cr}_2\text{O}_7^{2-}$ to CrO_4^{2-} (Eqs. (16) and (17))



and the reduction of CrO_4^{2-} (Eqs. (9), (12), and (15)). Also, the stoichiometries indicate that for the reduction of 1 mol Cr(VI), 1 mol of protons is necessary. The foregoing discussion summarized the stoichiometry of Cr(VI) reduction and protons consumption, that is, $[\text{Cr}(\text{VI})]_{\text{red}} = [\text{H}^+]_{\text{com}}$.

The pH of the solution is related to initial pH and protons consumption, which can be expressed in the following equation:

$$[\text{H}^+]_{\text{ini}} - [\text{H}^+]_{\text{com}} = [\text{H}^+]_{\text{fin}} \quad (18)$$

In which

$$[\text{H}^+]_{\text{com}} = [\text{Cr}(\text{VI})]_{\text{red}} = [\text{Cr}(\text{VI})]_{\text{ini}} - [\text{Cr}(\text{VI})]_{\text{fin}} \quad (19)$$

Substitute Eqs. (19) to (18), then we obtain:

$$[\text{H}^+]_{\text{ini}} - [\text{Cr}(\text{VI})]_{\text{ini}} + [\text{Cr}(\text{VI})]_{\text{fin}} = [\text{H}^+]_{\text{fin}} \quad (20)$$

The logarithmic style of Eq. (20) is

$$\lg([\text{H}^+]_{\text{ini}} - [\text{H}^+]_{\text{fin}}) = \lg([\text{Cr}(\text{VI})]_{\text{ini}} - [\text{Cr}(\text{VI})]_{\text{fin}}) \quad (21)$$

Assume that initial pH is in the range of 2–4 and final pH is neutral ($[\text{H}^+]_{\text{fin}} = 10^{-7}$), so $[\text{H}^+]_{\text{ini}} \gg 10^{-7}$, then Eq. (21) can be described as:

$$\lg([\text{Cr}(\text{VI})]_{\text{ini}} - [\text{Cr}(\text{VI})]_{\text{fin}}) = \lg [\text{H}^+]_{\text{ini}} \quad (22)$$

The concentration of Cr(VI) equals to zero by the end of EC process, which is $[\text{Cr}(\text{VI})]_{\text{fin}} = 0$.

Therefore, the final equation is:

$$-\lg [\text{Cr}(\text{VI})]_{\text{ini}} = -\lg [\text{H}^+]_{\text{ini}} = \text{pH}_{\text{ini}} \quad (23)$$

In our study, we defined the “p[Cr(VI)]” as chromic alkalinity, which was the quantitative capacity of Cr(VI) to neutralize an acid, and expressed as

$$\text{p}[\text{Cr}(\text{VI})] = -\lg [\text{Cr}(\text{VI})]_{\text{ini}} \quad (24)$$

On the other hand, “pH_f” was the solution pH value at the end-point of Cr(VI) removal.

Obviously, when $\text{p}[\text{Cr}(\text{VI})] = \text{pH}_i$, the final pH was neutral; $\text{p}[\text{Cr}(\text{VI})] < \text{pH}_i$, alkaline; and $\text{p}[\text{Cr}(\text{VI})] > \text{pH}_i$, acidic.

2.6. Experimental design

2.6.1. RSM experimental design

The 3-Level Factorial Design, a standard RSM, was selected for the evaluation of the factors which made sense on the final pH during Cr(VI) removal in EC process. In this design, three factors were the initial pH (x_1), initial Cr(VI) concentration (x_2) and current density (x_3), respectively [35]. All factors were controlled at three levels. The response variable (y) that represented final pH was fitted by a second-order model in the form of quadratic polynomial equation:

$$y = \beta_0 + \sum_{i=1}^m \beta_i x_i + \sum_{i < j}^m \beta_{ij} x_i x_j + \sum_{i=1}^m \beta_{ii} x_i^2 \quad (25)$$

where y is the response variable to be modeled, x_i and x_j are independent variables which determine y , β_0 , β_i and β_{ii} are the offset term, the i linear coefficient and the quadratic coefficient, respectively. β_{ii} is the term that reflect the interaction between x_i and x_j .

2.6.2. Batch experiments

Our study designed a serial of batch experiments to investigate the pH evolution in different final pH situations. Table 1 lists the detailed experimental conditions of the batch experiments. According to RSM experimental design, the initial Cr(VI) concentration was set in a range of 10–94 mg/L. The p[Cr(VI)] was calculated by Eq. (24).

3. Results and discussion

3.1. Significant factors for final pH

Table 2 shows the experimental matrix for three variables (Cr(VI) concentration, initial pH, and current density) and the corresponding experimental response. From the analysis of variance (ANOVA) of response surface quadratic model [35], the significant factors contributing to final pH were initial pH (F -value 305.01, “Prob > F ” less than 0.0001) and Cr(VI) concentration (F -value 28.53, “Prob > F ” less than 0.0001). Nevertheless, current density (F -value 0.012, “Prob > F ” 0.8917) was not significant.

Fig. 3a and b shows that final pH increases with increasing of the Cr(VI) concentration and initial pH, indicating a synergistic effect of these two variables on final pH. Similar studies also pointed out that final pH in aqueous solutions depends on the initial pH of the solution [6,7,20]. Indeed, it can be observed that the response surface in Fig. 3b is steeper than Fig. 3a, suggesting that the initial pH had a more significant impact on final pH than Cr(VI) concentration.

Fig. 3c indicates that final pH was conditioned by two variables, initial pH and Cr (VI) concentration. Additionally, final pH values were distributed over a wide range of acidic, neutral and alkaline zone, which confirmed our theory of Cr(VI) removal and pH evolution (Section 2.5.3). The relevance of these two variables (initial pH

Table 1
Experimental conditions applied in different final pH situations.

Cr(VI) (mg/L)	p[Cr(VI)] pH _i			
	p[Cr(VI)] = pH _i	p[Cr(VI)] < pH _i	p[Cr(VI)] > pH _i	
10	3.72	3.72	4.00	2.00
52	3.00	3.00	4.00	2.00
94	2.74	2.74	4.00	2.00

Table 2

Experimental matrix for natural variables and corresponding experimental response to final pH.

Std no.	Run no.	Cr(VI) (mg/L)	Initial pH	i (A/cm ²)	Final pH
1	29	10.00	2.00	0.010	2.19
2	8	52.00	2.00	0.010	2.81
3	16	94.00	2.00	0.010	3.03
4	22	10.00	3.00	0.010	5.51
5	28	52.00	3.00	0.010	7.60
6	21	94.00	3.00	0.010	10.93
7	23	10.00	4.00	0.010	10.04
8	13	52.00	4.00	0.010	11.02
9	1	94.00	4.00	0.010	11.31
10	24	10.00	2.00	0.025	2.12
11	25	52.00	2.00	0.025	2.53
12	11	94.00	2.00	0.025	2.96
13	20	10.00	3.00	0.025	5.63
14	12	52.00	3.00	0.025	7.66
15	15	94.00	3.00	0.025	10.97
16	17	10.00	4.00	0.025	9.92
17	27	52.00	4.00	0.025	11.09
18	26	94.00	4.00	0.025	11.31
19	14	10.00	2.00	0.040	2.13
20	30	52.00	2.00	0.040	2.77
21	5	94.00	2.00	0.040	3.05
22	19	10.00	3.00	0.040	5.73
23	3	52.00	3.00	0.040	7.95
24	10	94.00	3.00	0.040	11.02
25	6	10.00	4.00	0.040	10.08
26	9	52.00	4.00	0.040	11.05
27	7	94.00	4.00	0.040	11.24
28	18	52.00	3.00	0.025	7.60
29	2	52.00	3.00	0.025	7.72
30	4	52.00	3.00	0.025	7.82

and Cr(VI) concentration) on pH evolution would be discussed later (Section 3.2).

3.2. Effect of $p[\text{Cr(VI)}]$ and initial pH to pH evolution

3.2.1. $p[\text{Cr(VI)}] = \text{pH}_i$

According to the features of Cr(VI) removal rate (Fig. 4a), EC process was divided into four periods: rapid removal stage (I), constant removal stage (II), decelerating removal stage (III) and complete removal stage (IV).

During the stage I, we noticed that the super-faradaic dissolution (the dissolved total iron at regular intervals greater than that calculated by Faraday's law (Δm_{theo}) [23,36] happened, as shown in Fig. 4a. Note that chemical reduction by Fe(II) is the predominant route for Cr(VI) removal in Fe-EC process [7,14,16,20,30,31]. Additionally, according to the Cr-Pourbaix diagram [37], the cathode reduction of Cr(VI) to Cr(III) (Eqs. (10)–(12)) is thermodynamically favored under acidic conditions due to an increase of its standard potential with proton concentration [3]. Meanwhile, zero-valent iron reduction (Eqs. (13)–(15)) may occur at the anode surface due to the strong acidic pH conditions [3,4]. Thus, it was expected that such rapid Cr(VI) removal efficiency would be caused by the combined effect of chemical, cathode and zero-valent iron reduction. In stage II, the cathode reduction and zero-valent iron reduction had no apparent favorable effect on the removal of Cr(VI) since the solution pH was increasing [16]. Note that the dissolved total iron was equal to that calculated by Faraday's law (Δm_{theo}), it could be expected that chemical reduction becomes the major route of the Cr(VI) removal [3,38]. This process could be formulated in terms of two steps: ferrous dissolution (Eqs. (26), (27)) and Cr(VI) reduction (Eqs. (28) and (29)) [30,39].



$$v_1 = -d[\text{Fe(II)}]/dt = I/(nFV) \quad (27)$$

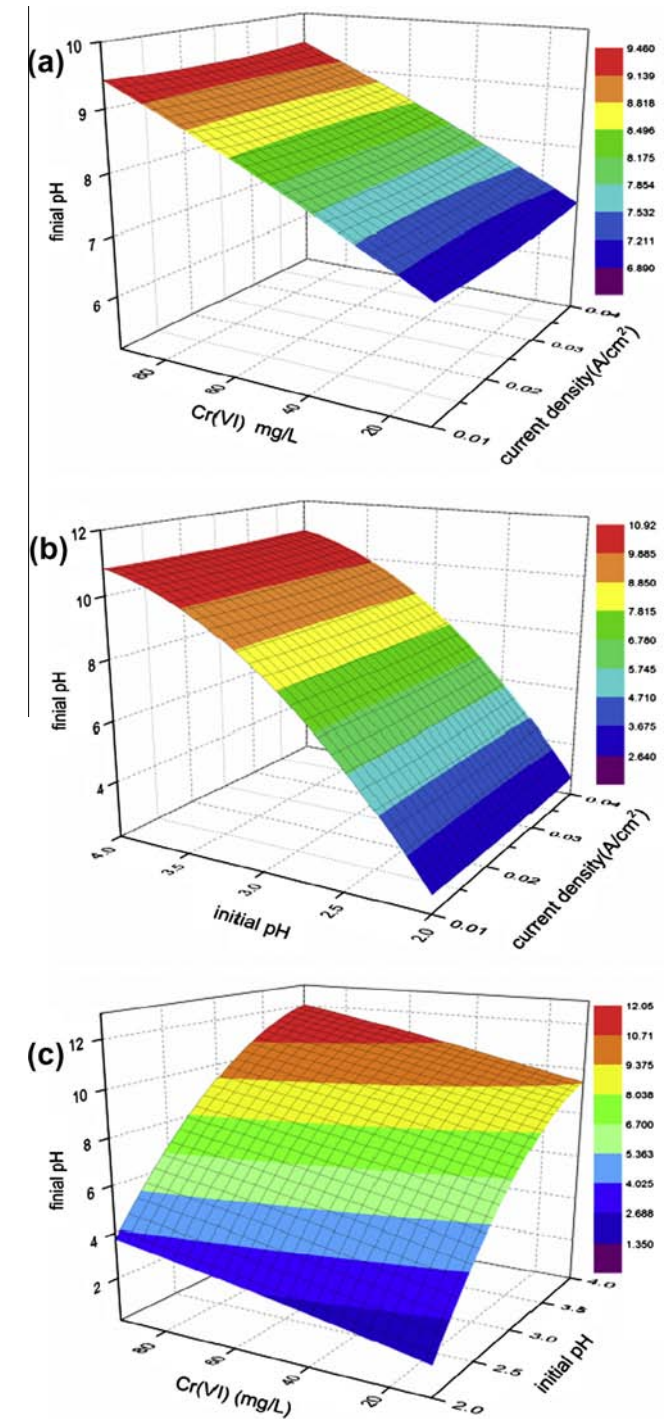
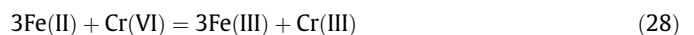


Fig. 3. The quadratic models of 3-Level Factorial Design: (a) Cr(VI) and current density; (b) initial pH and current density and (c) Cr(VI) and initial pH on final pH.



$$v_2 = -d[\text{Cr(VI)}]/dt = k[\text{Fe(II)}][\text{Cr(VI)}] \quad (29)$$

where v_1 and v_2 are the rate of Fe(II) generation and Cr(VI) reduction (mol/(L s)) respectively; I is the current (A); n is the number of electron moles ($n=2$, in Eq. (2)), F is the Faraday's constant ($F=96,487$ C/mol), V is the volume of solution (2.5 L), k is the pH-dependent rate coefficient.

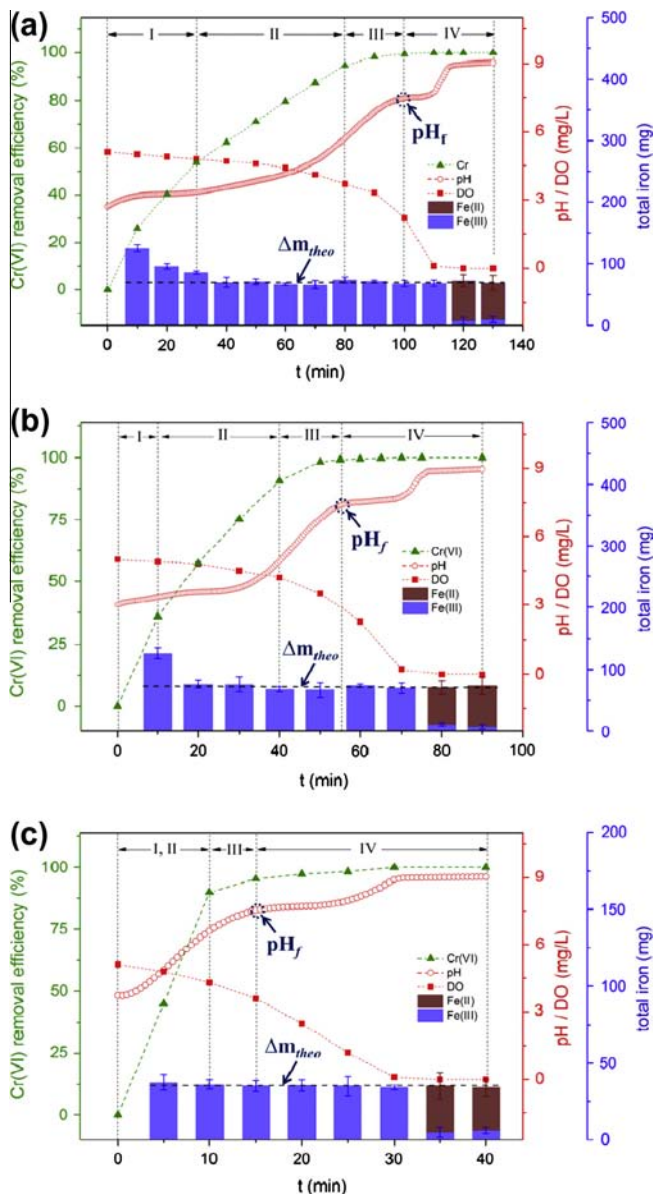
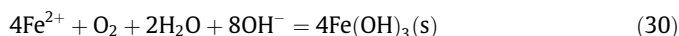


Fig. 4. The changes of Cr(VI) removal efficiency, pH, DO, and total iron at $p[Cr(VI)] = pH_i$: (a) initial Cr(VI) 94 mg/L, pH_i 2.74; (b) initial Cr(VI) 52 mg/L, pH_i 3.00; and (c) initial Cr(VI) 10 mg/L, pH_i 3.72. “ Δm_{theo} ” is the amounts of dissolved iron at regular intervals calculated by Faraday’s law. “ pH_f ” is pH value at the end of Cr(VI) removal.

During stage II, considering Cr(VI) removal rate almost constant, it was reasonable to suggest that ferrous dissolution was the rate-determining step ($\nu_1 < 3\nu_2$) of Cr(VI) removal in EC process.

In stage III, the gradual decrease of Cr(VI) in solution caused a drop in reaction rate of Eq. (29) [40]. Thereafter, the Cr(VI) reduction (Eq. (29)) became the rate-determining step ($\nu_1 > 3\nu_2$). Simultaneously, a significant increase of pH (from 5.0 to 7.0) and decrease of DO (from 3.8 to 2.2) were observed. Previous published experiments showed that the rate of Fe^{2+} oxidation by DO increases sharply with increasing pH (Eqs. (30) and (31)) [41,42]. Approximately 80% Fe^{2+} is oxidized in <10 min at pH 7.5, while at pH 6.5 it takes approximately 300 min (5 h) for the same oxidation to occur [43].



$$\nu_3 = -d[Fe(II)]/dt = k[Fe(II)][OH^-]^2 p_{O_2} \quad (31)$$

Compliance with the above results, so that the Cr(VI) removal rate declined dramatically in this stage ascribing to that oxygen would limit Cr(VI) reduction at very low Cr(VI) concentrations and very high pH values. Complementarily, the pH point marked with a circle in Fig. 4a represented the end of Cr(VI) removal and was known as the “final pH”.

During stage IV, the solution pH was first observed constant at 7.0 where the ferrous was oxidized by DO (Eq. (30)) simultaneously (Fig. 4a). As shown, the species of Fe(III) predominantly existed as $Fe(OH)_3(s)$ at pH 6–12 (Fig. 2), which appeared to have no influence on pH variation. To better understand the reason for pH evolution during stage IV, pH variation versus Fe(II) and Fe(III) with no Cr(VI) containing was studied, and the results were shown in Fig. 5. As expected, pH value remained constant when $Fe(OH)_3(s)$ existed only in the solution (50–60 min in Fig. 5).

Nevertheless, there was a significant rise in pH to 9.0 because of the DO deficiency (Fig. 4a). Subsequently it remained at this maximum value (Fig. 4a). This process was also consistent with the results of pH variation versus Fe(II) (0–30 min in Fig. 5). The reason for pH increase in stage IV (Fig. 4a) had not been elaborated before, but we confirmed that the direct cause of pH increase was due to a certain percentage of Fe^{2+} species residual in solution. Additionally, with respect to pH above 9.0, Fe^{2+} species transferred into $Fe(OH)_2(s)$, resulting in a constant pH value.

The trend of four stages was similar among Fig. 4a–c. However, it had to be mention that the duration of stage I in Fig. 4b and c was shorter than Fig. 4a. Additionally, it became impossible to distinguish the stage I and II in Fig. 4c. This might be ascribed to an increase of initial pH from 3.00 (Fig. 4b) to 3.72 (Fig. 4c). As stated in our report previously, the effect of cathode reduction and zero-valent iron reduction weakened with increasing pH.

The above results well confirmed our deduction shown in Section 2.3 that under the situation of $p[Cr(VI)] = pH_i$, final pH is neutral. Nevertheless, the solution pH continuous increased to 9.0 since Fe^{2+} species residual in solution.

On the other hand, by monitoring the pH evolution, the point of final pH can be detected. Therefore, the electrolytic time for Cr(VI) completely removed could be controlled, which avoided the extensive current supply and iron dissolved.

3.2.2. $p[Cr(VI)] < pH_i$

The features of Cr(VI) removal rate of $p[Cr(VI)] < pH_i$ and $p[Cr(VI)] = pH_i$ were identical except for one detail: the decelerating removal stage (III) occurring before constant removal stage (II) in the situation of $p[Cr(VI)] < pH_i$. As shown in Fig. 6, concurrent

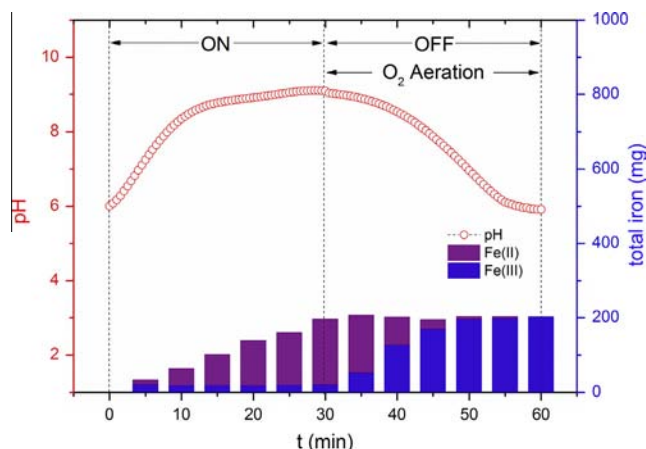


Fig. 5. pH variation versus Fe(II) and Fe(III) with no Cr(VI) containing: electrolyzing (ON) for 30 min; then ending electrolysis (OFF), and aerating oxygen for 30 min.

with increasing pH value to 7.0, reaction rate of Fe^{2+} by DO also increased by the end of stage I. Hence, a competition for ferrous might happen between Cr(VI) and DO, which resulted in Cr(VI) removal rate decrease. It had to be mentioned that the Cr(VI) removal rate herein (Fig. 6a) was higher than the value of stage (III) (Fig. 4a) in $p[\text{Cr(VI)}] = \text{pH}_i$ and the reason for this, as commented earlier, was the kinetics rate (v_2) with difference Cr(VI) concentration.

In stage I, there was no super-faradaic phenomenon, however, a rapid Cr(VI) removal rate was also observed (Fig. 6). Since zero-iron reduction rate would drop almost 75% when pH increased from 2.74 to 4.00 according to the zero-iron kinetics (Eq. (32)) [3,34], and thus, we assumed the main reason for this rapid Cr(VI) removal was due to the cathode reduction [32,33].

$$v_4 = -d[\text{Cr(VI)}]/dt = k_4[\text{Cr(VI)}]^{0.5}[\text{H}^+]^{0.5}(\text{Area}) \quad (32)$$

Similarly, the electrodisolution was the rate-determining step ($v_1 < 3v_2$) [40] and consequently resulted in the constant Cr(VI) removal rate in stage II (Fig. 6). On the other hand, the solution pH

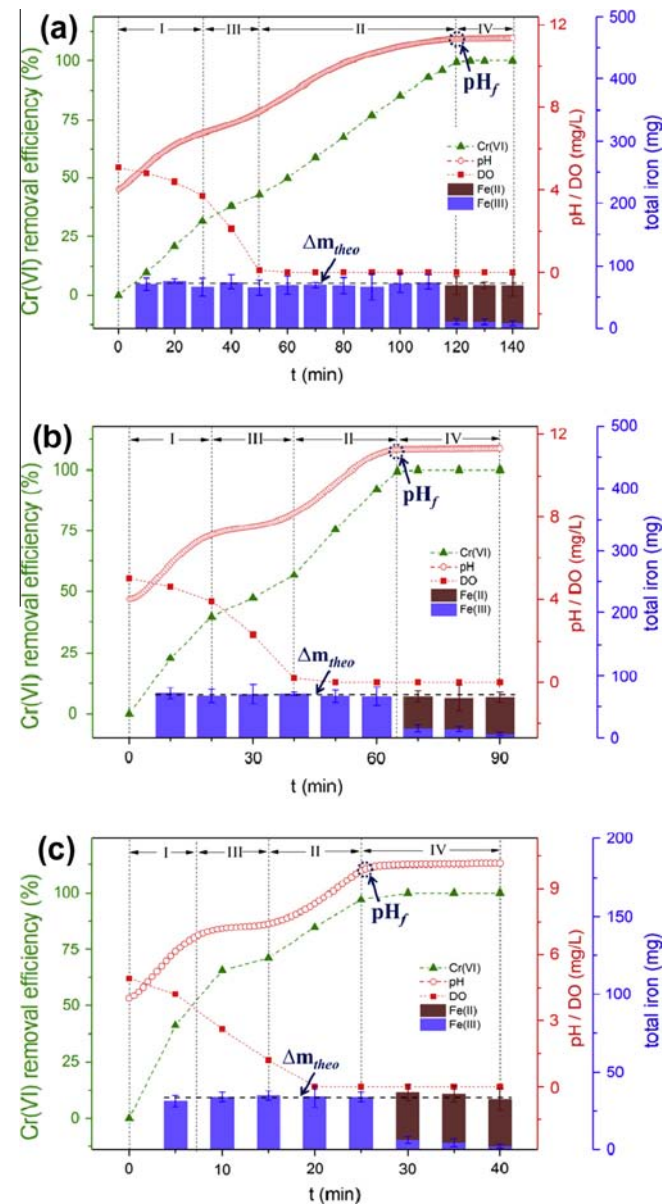


Fig. 6. The changes of Cr(VI) removal efficiency, pH, DO, and total iron at $p[\text{Cr(VI)}] < \text{pH}_i$: (a) initial Cr(VI) 94 mg/L, pH_i 4.00; (b) initial Cr(VI) 52 mg/L, pH_i 4.00; and (c) initial Cr(VI) 10 mg/L, pH_i 4.00.

remained relatively constant and equaled to final pH by the end of Cr(VI) removal in stage IV (Fig. 6). Therefore, a same conclusion was drawn from the pH monitored in EC systems: the terminal point of Cr(VI) removal can be detected by pH-invariant feature, which was expressed as $dpH/dt = 0$.

3.2.3. $p[\text{Cr(VI)}] > \text{pH}_i$

As seen qualitatively in Figs. 4, 6 and 7, the removal rate of Cr(VI) increased with decreasing initial pH. This was quantitatively by calculating the electrolytic time. For initial Cr(VI) concentration 92 mg/L, it took about 120, 100 and 75 min, respectively to completely remove Cr(VI) in the situations of $p[\text{Cr(VI)}] < \text{pH}_i$, $p[\text{Cr(VI)}] = \text{pH}_i$ and $p[\text{Cr(VI)}] > \text{pH}_i$. Hence, faster Cr(VI) removal

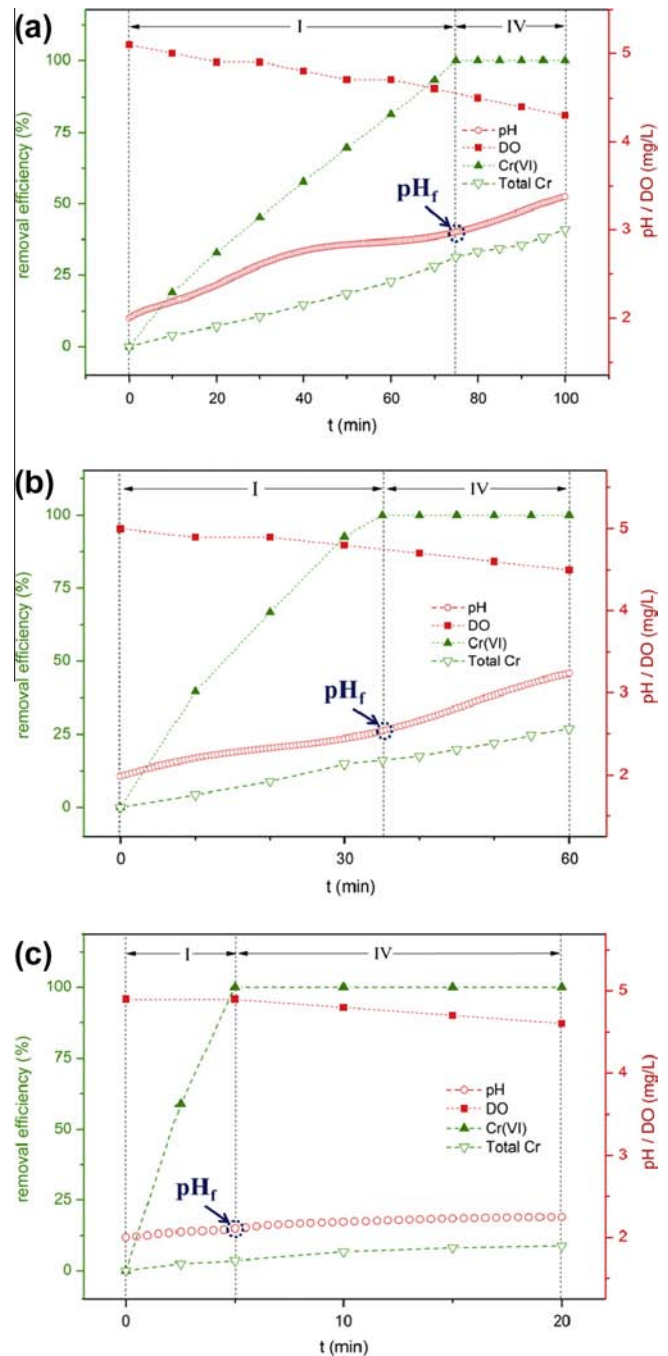


Fig. 7. The changes of Cr(VI) removal efficiency, pH, DO, and total iron at $p[\text{Cr(VI)}] > \text{pH}_i$: (a) initial Cr(VI) 94 mg/L, pH_i 2.00; (b) initial Cr(VI) 52 mg/L, pH_i 2.00; and (c) initial Cr(VI) 10 mg/L, pH_i 2.00.

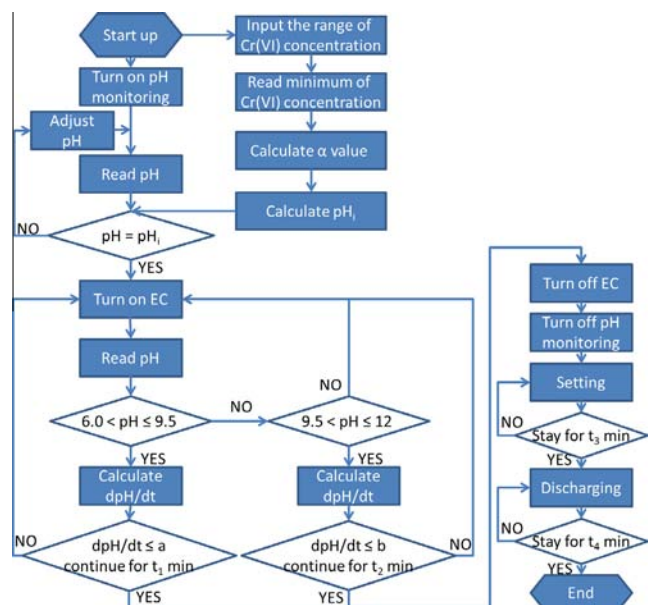


Fig. 8. Real-time control strategy of EC process. The values of a and b , and the time parameters of t_1 , t_2 , t_3 and t_4 are pre-established by experiments before using the control system.

rate was obtained by decreasing initial pH, which was consistent with our results earlier. Further to this, the solution pH during the whole EC process never exceeded to 4.5 and final pH was acidic (Fig. 7). As such, Cr(VI) removal rate remained relatively fast, and stage II and III subsequently disappeared in the EC process. In response to the lower initial pH value, there was a sharp continuous increase in final pH, which was consistent with previous results summarized in Section 3.2.1: the solution pH increased with increasing concentration of Fe(II) in acidic conditions. Therefore, the point of final pH was difficult to be detected by monitoring the pH evolution during EC process. Additionally, rapid Cr(VI) removal rate was achieved when $p[\text{Cr(VI)}] > p\text{H}_i$. However, the major fraction of dissolved Cr(III) was due to the acidic bulk solution [14,16,20].

3.3. Real-time control strategy

Based on the above results, an integrated real-time control scheme was proposed for fluctuant (or stable) Cr(VI)-containing wastewater (Fig. 8).

Before using the control system, the range of Cr(VI), the values of a and b , and the time parameters of t_1 , t_2 , t_3 and t_4 were pre-established by a series debugging experiments.

If the pH value in the solution was equivalent to $p[\text{Cr(VI)}]_{\min}$, then the EC process would be carried out. During the EC process, digital signals of pH were collected at 30 s intervals and smoothed by the moving average filter. If $dp\text{H}/dt \leq a$ lasted for t_1 min in the pH range of 6.5–9.5, it indicated that Cr(VI) was removed completely (based on the features of pH evolution when $p[\text{Cr(VI)}] = p\text{H}_i$). Otherwise, read pH continuously, if pH was in the range of 9.5–12.5 and $dp\text{H}/dt \leq b$ simultaneously lasted for t_2 min, implying Cr(VI) reduced completely (based on the features of pH evolution when $p[\text{Cr(VI)}] < p\text{H}_i$), then the EC and pH monitoring system would be stopped and next settling and discharge stages would be activated.

4. Conclusions

Our research identified key parameters that influence the final pH of EC process. The final pH was influenced by initial pH and

initial Cr(VI) concentration rather than by current density. Additionally, the relations between them was that when $p[\text{Cr(VI)}] = p\text{H}_i$, the final pH was neutral; when $p[\text{Cr(VI)}] < p\text{H}_i$, the final pH was alkaline; and when $p[\text{Cr(VI)}] > p\text{H}_i$, the final pH was acidic.

From the serial studies of $p[\text{Cr(VI)}]$ and initial pH, four periods (rapid removal stage, constant removal stage, decelerating removal stage and complete removal stage) were divided according to the rate of Cr(VI) removal.

At stage I, a rapid Cr(VI) removal efficiency was achieved by the combined effects of chemical, cathode and zero-valent iron reduction. For stage II, a constant Cr(VI) removal rate occurred was due to the rate-determining step ($v_1 < 3v_2$) of ferrous dissolution. Oxygen would limit Cr(VI) reduction in the conditions of low Cr(VI) concentration and high pH, thus causing a decelerating removal efficiency in stage III. Overall Cr(VI) removal was completed when the final pH was reached in the last stage.

The point of final pH can be detected by the features of pH evolution in the case of $p[\text{Cr(VI)}] = p\text{H}_i$ and $p[\text{Cr(VI)}] < p\text{H}_i$. Rapid Cr(VI) removal rate was achieved when $p[\text{Cr(VI)}] > p\text{H}_i$. However, the major fraction of Cr(III) was still dissolved and the point of final pH was difficult to be detected in this condition.

Thereafter, we proposed a real-time control strategy for fluctuant (or stable) Cr(VI)-containing wastewater treatment.

Acknowledgements

We are grateful for the National Key Science and Technology Project for Water Environmental Pollution Control (2009ZX07212-001-02), the financial support of the National Natural Science Foundation of China (30970105).

References

- [1] Commission of the European Communities, Directive 2000/60/EC of the European Parliament and of the Council of 23 October 2000 establishing a framework for Community action in the field of water policy, Office for Official Publications of the European Communities, 2000.
- [2] C.E. Barrera-Diaz, V. Lugo-Lugo, B. Bilyeu, A review of chemical, electrochemical and biological methods for aqueous Cr(VI) reduction, *J. Hazard. Mater.* 223 (2012) 1–12.
- [3] A.K. Golder, A.K. Chanda, A.N. Samanta, S. Ray, Removal of hexavalent chromium by electrochemical reduction-precipitation: investigation of process performance and reaction stoichiometry, *Sep. Purif. Technol.* 76 (2011) 345–350.
- [4] E. Keshmirizadeh, S. Yousefi, M.K. Rofouei, An investigation on the new operational parameter effective in Cr(VI) removal efficiency: a study on electrocoagulation by alternating pulse current, *J. Hazard. Mater.* 190 (2011) 119–124.
- [5] I. Heidmann, W. Calmano, Removal of Ni, Cu and Cr from a galvanic wastewater in an electrocoagulation system with Fe- and Al-electrodes, *Sep. Purif. Technol.* 71 (2010) 308–314.
- [6] M.S. Bhatti, A.S. Reddy, A.K. Thukral, Electrocoagulation removal of Cr(VI) from simulated wastewater using response surface methodology, *J. Hazard. Mater.* 172 (2009) 839–846.
- [7] G. Mouedhen, M. Feki, M. De Petris-Wery, H.F. Ayedi, Electrochemical removal of Cr(VI) from aqueous media using iron and aluminum as electrode materials: towards a better understanding of the involved phenomena, *J. Hazard. Mater.* 168 (2009) 983–991.
- [8] P. Gao, X.M. Chen, F. Shen, G.H. Chen, Removal of chromium(VI) from wastewater by combined electrocoagulation–electroflotation without a filter, *Sep. Purif. Technol.* 43 (2005) 117–123.
- [9] A. Mahmoud, A.F.A. Hoadley, An evaluation of a hybrid ion exchange electro dialysis process in the recovery of heavy metals from simulated dilute industrial wastewater, *Water Res.* 46 (2012) 3364–3376.
- [10] J. Zhao, G. Cui, H. Liu, Investigation into rejuvenation of spent chromium plating solutions by bipolar membrane electro dialysis, *J. Electrochem. Soc.* 158 (2011) D561–D566.
- [11] L. Alvarado, A. Ramírez, I. Rodríguez-Torres, Cr(VI) removal by continuous electrodeionization: study of its basic technologies, *Desalination* 249 (2009) 423–428.
- [12] L. Alvarado, I.R. Torres, A. Chen, Integration of ion exchange and electrodeionization as a new approach for the continuous treatment of hexavalent chromium wastewater, *Sep. Purif. Technol.* 105 (2013) 55–62.
- [13] http://www.english.gov.cn/wwwHome/201108/t20110807_382764.htm (08/2011); Comprehensive treatment of heavy metal pollution of Xiangjiang river.

- [14] I. Heidmann, W. Calmano, Removal of Cr(VI) from model wastewaters by electrocoagulation with Fe electrodes, *Sep. Purif. Technol.* 61 (2008) 15–21.
- [15] T. Olmez, The optimization of Cr(VI) reduction and removal by electrocoagulation using response surface methodology, *J. Hazard. Mater.* 162 (2009) 1371–1378.
- [16] M.G. Arroyo, V. Perez-Herranz, M.T. Montanes, J. Garcia-Anton, J.L. Guinon, Effect of pH and chloride concentration on the removal of hexavalent chromium in a batch electrocoagulation reactor, *J. Hazard. Mater.* 169 (2009) 1127–1133.
- [17] K.C. Chen, C.Y. Chen, J.W. Peng, J.Y. Houg, Real-time control of an immobilized-cell reactor for wastewater treatment using ORP, *Water Res.* 36 (2002) 230–238.
- [18] J.H. Kim, M. Chen, N. Kishida, R. Sudo, Integrated real-time control strategy for nitrogen removal in swine wastewater treatment using sequencing batch reactors, *Water Res.* 38 (2004) 3340–3348.
- [19] S.G. Won, C.S. Ra, Biological nitrogen removal with a real-time control strategy using moving slope changes of pH(mV)- and ORP-time profiles, *Water Res.* 45 (2011) 171–178.
- [20] P. Lakshmiathiraj, G.B. Raju, M.R. Basariya, S. Parvathy, S. Prabhakar, Removal of Cr (VI) by electrochemical reduction, *Sep. Purif. Technol.* 60 (2008) 96–102.
- [21] K. Dermentzis, A. Christoforidis, E. Valsamidou, A. Lazaridou, N. Kokkinos, Removal of hexavalent chromium from electroplating wastewater by electrocoagulation with iron electrodes, *Global Nest J.* 13 (2011) 412–418.
- [22] G. Mouedhen, M. Feki, M.D.P. Wery, H.F. Ayedi, Behavior of aluminum electrodes in electrocoagulation process, *J. Hazard. Mater.* 150 (2008) 124–135.
- [23] D. Lakshmanan, D.A. Clifford, G. Samanta, Ferrous and ferric ion generation during iron electrocoagulation, *Environ. Sci. Technol.* 43 (2009) 3853–3859.
- [24] A.D. Eaton, L.S. Clesceri, A.E. Greenberg, M.A.H. Franson, A.P.H. Association, A.W.W. Association, W.E. Federation, Standard Methods for the Examination of Water and Wastewater, American Public Health Association, 1998.
- [25] A.I. Vogel, A Text-Book of Quantitative Inorganic Analysis, Including Elementary Instrumental Analysis, Longmans, 1961.
- [26] J. Gustafsson, Visual MINTEQ version 3.0, KTH Royal Inst. of Technol., Stockholm, Sweden, 2010.
- [27] R. Smith, A. Martell, R. Motekaitis, NIST standard reference database 46, NIST Critically Selected Stability Constants of Metal Complexes Database Ver, 7.0, 2003.
- [28] J.P. Gustafsson, I. Persson, D.B. Kleja, J.W.J. van Schaik, Binding of iron(III) to organic soils: EXAFS spectroscopy and chemical equilibrium modeling, *Environ. Sci. Technol.* 41 (2007) 1232–1237.
- [29] H.A. Moreno, D.L. Cocke, J.A.G. Gomes, P. Morkovsky, J.R. Parga, E. Peterson, C. Garcia, Electrochemical reactions for electrocoagulation using iron electrodes, *Ind. Eng. Chem. Res.* 48 (2009) 2275–2282.
- [30] I.J. Buerge, S.J. Hug, Kinetics and pH dependence of chromium(VI) reduction by iron(II), *Environ. Sci. Technol.* 31 (1997) 1426–1432.
- [31] N. Adhoum, L. Monser, N. Bellakhal, J.E. Belgaied, Treatment of electroplating wastewater containing Cu^{2+} , Zn^{2+} and Cr(VI) by electrocoagulation, *J. Hazard. Mater.* 112 (2004) 207–213.
- [32] M.S. Bhatti, A.S. Reddy, R.K. Kalia, A.K. Thukral, Modeling and optimization of voltage and treatment time for electrocoagulation removal of hexavalent chromium, *Desalination* 269 (2011) 157–162.
- [33] C. Barrera-Diaz, V. Lugo-Lugo, G. Roa-Morales, R. Natividad, S.A. Martinez-Delgado, Enhancing the electrochemical Cr(VI) reduction in aqueous solution, *J. Hazard. Mater.* 185 (2011) 1362–1368.
- [34] J.P. Gould, The kinetics of hexavalent chromium reduction by metallic iron, *Water Res.* 16 (1982) 871–877.
- [35] J. Huang, Z.H. Yang, G.M. Zeng, M. Ruan, H.Y. Xu, W.C. Gao, Y.L. Luo, H.M. Xie, Influence of composite flocculant of PAC and MBFGA1 on residual aluminum species distribution, *Chem. Eng. J.* 191 (2012) 269–277.
- [36] P. Cañizares, F. Martínez, C. Jiménez, J. Lobato, M.A. Rodrigo, Coagulation and electrocoagulation of wastes polluted with dyes, *Environ. Sci. Technol.* 40 (2006) 6418–6424.
- [37] M. Pourbaix, Atlas of Electrochemical Equilibria in Aqueous Solutions, National Association of Corrosion Engineers, 1974.
- [38] H. Cui, Y. Qian, H. An, C. Sun, J. Zhai, Q. Li, Electrochemical removal of fluoride from water by PAOA-modified carbon felt electrodes in a continuous flow reactor, *Water Res.* 46 (2012) 3943–3950.
- [39] D.L. Sedlak, P.G. Chan, Reduction of hexavalent chromium by ferrous iron, *Geochim. Cosmochim. Acta* 61 (1997) 2185–2192.
- [40] S.E. Fendorf, G. Li, Kinetics of chromate reduction by ferrous iron, *Environ. Sci. Technol.* 30 (1996) 1614–1617.
- [41] W. Stumm, G.F. Lee, Oxygenation of ferrous iron, *Ind. Eng. Chem.* 53 (1961) 143–146.
- [42] W. Stumm, J.J. Morgan, Aquatic Chemistry: Chemical Equilibria and Rates in Natural Waters, Wiley, 1996.
- [43] B. Morgan, O. Lahav, The effect of pH on the kinetics of spontaneous Fe(II) oxidation by O_2 in aqueous solution-basic principles and a simple heuristic description, *Chemosphere* 68 (2007) 2080–2084.